ChemComm

COMMUNICATION

View Article Online
View Journal | View Issue

Cite this: *Chem. Commun.*, 2019, 55, 12463

Received 30th August 2019,
Accepted 18th September 2019

DOI: 10.1039/c9cc06738h

rsc.li/chemcomm

LAMP-generated H^+ ions-induced dimer i-motif as signal transducer for ultrasensitive electrochemical detection of DNA†

Xiaoyu Hua, Enfen Yang, Wenting Yang, Ruo Yuan * and Wenju Xu *

Herein, an ultrasensitive electrochemical biosensor is proposed for the quantification of the Flu A virus biomarker DNA (fDNA), and is based on loop-mediated isothermal amplification-generated hydrogen ions (LAMP-H^+) which induce the formation of the dimer i-motif structure (DiMS) for signal transduction, coupled with exonuclease III (ExoIII)-assisted DNA walking for signal dual-amplification.

Loop-mediated isothermal amplification (LAMP), pioneered by Notomi's group in 2000, is a powerful technique of nucleic acid amplification due to the advantages of rapidness, convenience, specificity and high efficiency, and in the method, with the help of Bst polymerase, the targeted nucleic acid template can be isothermally amplified to 10^9 copies or more in an hour or less.[1,2] In the last few decades, typical examples of LAMP application were involved in the detection of different biomolecules, such as genes, viruses and bacteria.[3–5] Whereas, the real-time or end-point quantitative technologies employed to identify LAMP products such as fluorescence staining, electrophoresis, colorimetry or turbidity, usually suffered from low quantitative sensitivity, narrow linear ranges, false-positive signals and intrinsic complexity.[6–10] These visual methods performed using the naked eye were somewhat subjective, inevitably leading to inaccurate quantification with low sensitivity, especially for those targets at the ultratrace level. Recently, we used a handy and portable pH meter to directly monitor the activity variation of the end-point by-product H^+ ions generated in LAMP (LAMP-H^+), achieving rapid determination of *Nosema bombycis genomic PTP1*.[11] Nevertheless, the analytical sensitivity was still insufficient because of the limited capability of the pH meter which only responded to 0.001 pH variations. Therefore, it is of great significance to explore more sensitive methods for the reliable detection of nucleic acid analytes as LAMP templates. Interestingly, the indirect assay of PTP1-templated LAMP with improved sensitivity has been developed through PTP1-dependent LAMP-H^+ regulating the conformational switch of a pH-responsive DNA nanostructure to obtain the sensitive electrochemical response of ferrocene (Fc).[12] Unfortunately, the insufficient sensitivity due to the absence of signal amplification strategies still restricts the applicability of the LAMP technique in quantifying some ultratrace analytes of interest. Here, the rational and subtle combination of LAMP-H^+ and diverse functional DNA nanostructures (*i.e.* i-motifs) with pH-responsiveness will offer great inspiration and accessibility to explore ultrasensitive electrochemical methods by introducing a signal dual-amplification scheme.

As a special DNA quadruplex, i-motif structures (iMSs) formed at weakly acidic conditions are possibly tethered in one, two, or four DNA strands through semi-protonated C·CH^+ pairs, corresponding to intramolecular, dimer or tetramer iMSs, respectively.[13–15] As expected, the high-dependence of the iMS on pH can offer a wide variety of applications for iMSs in pH sensors,[16] delivery systems,[17] and switchable nanodevices.[18] In particular, the easy modification and facile labeling endow iMSs with additional possibilities to be specific signal transducers for the construction of various biosensors.[19] Through the detectable signal conversion scheme, some of them can monitor pH changes inside living cells and organisms.[15,20,21] Furthermore, Nesterova and co-workers demonstrated that the response sensitivity and transition midpoint of iMSs could be precisely regulated over a physiologically relevant pH interval.[22] Thus, pH-responsive iMSs could provide great potential to probe the LAMP-H^+ variation, specifically through the elaborate combination of signal transduction and signal amplification. Therefore, it would lead to innovative development of ultrasensitive electrochemical methods for biomolecule detection.

Herein, based on a LAMP-H^+-induced dimer iMS (DiMS) as the signal transducer and ExoIII-assisted DNA walking as the signal amplifier, an ultrasensitive electrochemical biosensor was reported to detect Flu A virus biomarker DNA (fDNA). As schematically illustrated in Scheme 1, the key conception of our method is ascribed to the rational and subtle combination of

Key Laboratory of Luminescent and Real-Time Analytical Chemistry (Southwest University), Ministry of Education, School of Chemistry and Chemical Engineering, Southwest University, Chongqing 400715, P. R. China. E-mail: xwju@swu.edu.cn, yuanruo@swu.edu.cn

† Electronic supplementary information (ESI) available: Experimental details and supplementary figures and tables. See DOI: 10.1039/c9cc06738h

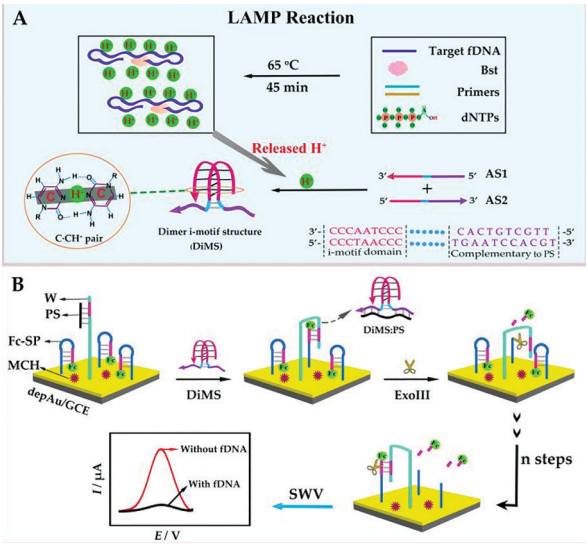

Scheme 1 Schematic diagrams of (A) releasing of hydrogen ions in fDNA-templated LAMP (LAMP-H$^+$) and the formation of the pH-responsive dimer i-motif structure (DiMS) induced by LAMP-H$^+$ through C·CH$^+$ pairs of AS1 and AS2, and (B) fabrication of the electrochemical biosensor based on DiMS as signal transducer and ExoIII-assisted W walking for signal dual-amplification.

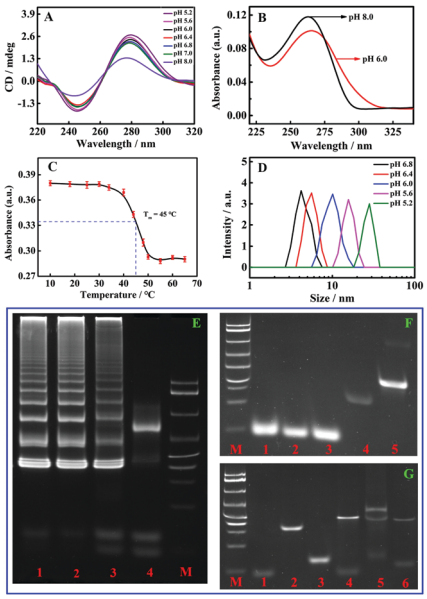

Fig. 1 (A) CD spectra, (B) UV-Vis spectra, (C) thermal stability and (D) DLS of DiMSs formed at different pH values. The concentration of both AS1 and AS2 was 500 nM. (E, F and G) PAGE images at different conditions compared with a DNA ladder with DNA-markers of 25, 50, 75, 100, 150, 200, 300, 400 and 500 bp (lane M): (E) LAMP reactions with different concentrations of fDNA, 100 ng μL^{-1} (lane 1), 1.0 ng μL^{-1} (lane 2), 10 pg μL^{-1} (lane 3) and 1.0 fg μL^{-1} (lane 4); (F) DiMS formation: PS (lane 1), AS1 (lane 2), AS2 (lane 3), DiMS (lane 4), and DiMS + PS (lane 5). (G) DNA reactions at the electrode surface: PS (lane 1), W (lane 2), Fc-SP (lane 3), PS + W (lane 4), Fc-SP + W (lane 5) and Fc-SP + W + ExoIII (lane 6). The pH of the 1× TBE buffer for (E) and (G) was 8.0, and for (F) was 6.5. The concentrations of all DNA samples and ExoIII were 2 μM and 10 U, respectively. Error bars: standard deviation (*s*), n = 5.

signal transduction and signal dual-amplification, in which the target fDNA is translated by LAMP-H$^+$ into the amplified current response of ferrocene (Fc). Firstly, the formation of DiMS with pH-dependence was triggered by LAMP-H$^+$ through semi-protonated C·CH$^+$ pairs of two affinity strands. Then, the overhang tails in DiMS cooperatively hybridized with a protection strand to release a DNA walker (W). Subsequently, the released W in turn unfolded Fc-tagged hairpin signal probes (Fc-SP), allowing for the formation of a blunt duplex close to 3′-terminus of Fc-SP. When introducing ExoIII, the opened Fc-SP was cleaved at ExoIII-recognizable sites of the duplex, accompanied by the throwing away of Fc from the electrode and the release of W.[23] As a result, the significantly decreased electrochemical signal could be utilized to quantify the target fDNA. This strategy paves a promising avenue for the electrochemical detection of biomolecules and holds great potential for the diagnosis and treatment of different diseases.

Schemes S1 and S2 in the ESI† schematically illustrate the H$^+$ generation during the LAMP reaction and the working principle, and show pictures of the two solutions after LAMP reaction in the absence (−) and presence (+) of fDNA with white precipitates of magnesium pyrophosphate (the inset in Scheme S1, ESI†). Moreover, CD spectra of DiMS assembled at different pHs (5.2, 5.6, 6.0, 6.4, 6.8, 7.0 and 8.0) were recorded. From Fig. 1A, a strong positive peak near 285 nm and a smaller negative peak near 255 nm are observed in the pH range from 5.2 to 7.0, attributed to the specific absorptions of i-motifs in CD spectra.[24] On increasing the pH to 8.0, the positive and negative peaks shifted to near 270 and 245 nm, suggesting the dissociation of DiMS under weakly alkaline conditions.[25] These observations demonstrated that the DiMS could be stabilized at pHs lower than 7.0 down to 5.2.[26] The UV-Vis spectra of the DiMS at pH 6.0 and 8.0 are shown in Fig. 1B. On changing the pH from 6.0 to 8.0, the obvious variation and slight blue shift of the characteristic absorption peak suggested that the DiMS was disassembled into DNA single strands.[18,19] These observations suggested that a stable DiMS maintained in a slightly acidic environment would undergo a configuration switch from i-motif to random coil at certain basic pHs. The thermal stability (T_m) of the DiMS at pH 6.0 was also investigated by measuring UV-Vis absorbance peaks at 295 nm at different temperatures.[21] From Fig. 1C, on increasing the solution temperature from 10 to 35 °C, almost no change of the UV-Vis absorbance was observed, and subsequently the absorption sharply decreased at temperatures higher than 40 °C and leveled off at about 50 °C. According to the T_m definition as the midpoint of the absorbance change,[24] the T_m of our DiMS was estimated to be 45 °C, suggesting its sufficient stability at room temperature, which is desirable for electrode fabrication and experimental measurements. The dynamic light scattering (DLS) result shown in Fig. 1D revealed that the hydrodynamic sizes of the dispersed DiMS increased with decreasing pH.[27,28] The atomic force microscope (AFM) images of the DiMS at different pH values are shown in Fig. S1 (ESI†). With the help of the fluorescence change of the DiMS at different pH values, the dependent relationship between DiMS and LAMP-H$^+$ was demonstrated (Fig. S2, ESI†). Fig. 1E–G depict

the polyacrylamide gel electrophoresis (PAGE) of different DNA samples, including the LAMP reactions with different concentrations of fDNA, DiMS formation and DNA reactions at the electrode surface. The oligonucleotide sequences are listed in Table S1 (ESI†). Obviously, ladder-like multiple bands with decreased concentration of fDNA were observed (lane 1–4 in Fig. 1E). Compared with intact PS, AS1 and AS2 (lane 1, 2 and 3 in Fig. 1F), the formed DiMS showed its characteristic mobility (lane 4) and the hybridized DiMS:PS gave a slower band (lane 5). From Fig. 1G, lane 1 and 2, respectively, are attributed to the PAGE bands of single PS and W, and a significantly lowered mobility (lane 4) was observed after their complementary hybridization. Upon treatment of W with Fc-SP (lane 3), a distinctly slower band was observed (lane 5), indicating the hybridization between W and unfolded Fc-SP. In the presence of ExoIII, a slow mobility band with a relatively wide range was produced (lane 6) due to the cleavage of unfolded Fc-SP. As expected, these results demonstrated the successful hybridization reactions of different DNA samples.

Under the optimized conditions (Fig. S3, ESI†), the stepwise fabrication of this biosensor was characterized by cyclic voltammetry (CV) (Fig. 2A) and electrochemical impedance spectroscopy (EIS) (Fig. 2B) measured in 5 mM $[Fe(CN)_6]^{4-/3-}$. Upon electrodeposition of bare GCE (curve a) in 1% $HAuCl_4$, the CV signal greatly increased and the EIS signal (R_{et}) decreased (curve b). After the incubation of Fc-SP′ and hybridized PS and W, significantly a decreased CV response and increased EIS plot were observed (curve c). The next addition of MCH as a blocking agent led to similar CV and EIS changes (curve d). When the as-formed DiMS and ExoIII were introduced, successively increasing CV signal and decreasing EIS plots were obtained (curve e and f). This was because of the occurrence of three continuous and overlapping processes, involving in DiMS taking off PS to release W, Fc-SP′ unfolding and ExoIII-recognizable cleavage to promote W walking, which greatly enhanced the electron transfer of $[Fe(CN)_6]^{4-/3-}$. These observations demonstrated well the reliable electrochemical behaviour of this biosensor to probe the fDNA concentration based on a LAMP-H^+ induced pH-responsive DiMS for signal transduction and ExoIII-assisted W walking for signal dual-amplification. Meanwhile, the square wave voltammetry (SWV) response of five electrodes (b, c, d, e and f) was also measured in PBS (pH 7.0). As we can see from Fig. 2C, the electrode depAu/GCE hardly gave a SWV signal in the absence of electron mediator Fc (curve b). After immobilizing Fc-SP and hybridized

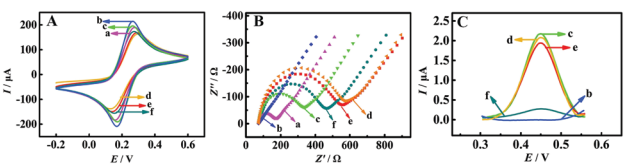

Fig. 2 (A) CV and (B) EIS response of different modified electrodes: (a) GCE, (b) depAu/(a), (c) Fc-SP′ + W:PS/(b), (d) MCH/(c), (e) DiMS/(d), and (f) ExoIII/(e). (C) SWV response of electrodes: (b) depAu/(a), (c) Fc-SP + W:PS/(b), (d) MCH/(c), (e) DiMS/(d), and (f) ExoIII/(e). The concentration of fDNA was 100 ng μL^{-1}.

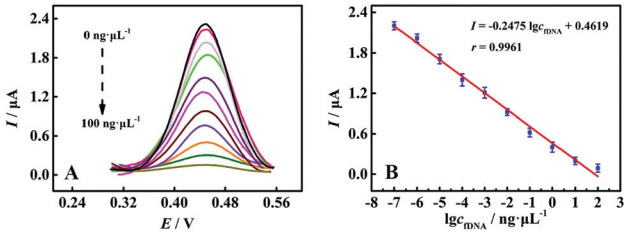

Fig. 3 (A) SWV response of the biosensor to different concentrations of fDNA: 0, 0.1, 1.0, 10, 100 fg μL^{-1}, 1.0, 10, 100 pg μL^{-1}, 1.0, 10, 100 ng μL^{-1}. (B) The linear calibration curve plotting SWV peak current I (μA) at +0.45 V peak voltage *vs.* the logarithm of fDNA concentration (ng μL^{-1}). Error bars: *s*, n = 5.

PS and W, a significantly increased SWV response was obtained (curve c), followed by a successive decrease upon incubation of MCH, DiMS and ExoIII (curve d, e and f).

Under the optimal conditions, the SWV responses of the biosensor to different concentrations of fDNA were examined. As illustrated in Fig. 3A, the SWV signal gradually decreased with increasing fDNA concentration in LAMP. Fig. 3B shows the resultant linear calibration curve plotting the SWV peak current (I μA) corresponding to fDNA concentrations in the range of 0.1 fg μL^{-1} to 100 ng μL^{-1}. Obviously, a good linear relationship was obtained with a regression equation of I (μA) = $-0.2475 \lg c_{fDNA} + 0.4619$ and a correlation coefficient (r) of 0.9961. The limit of detection (LOD) of this biosensor was determined according to the equation ($I_L = I_0 + ks_B$) provided by IUPAC,[29] where I_0 and s_B are the SWV signal and the standard deviation of the blank sample, respectively. As suggested by IUPAC, coefficient k generally equaled 3 to allow a confidence level of 99.9%. In our experiment, I_0 and s_B of five parallel measurements were 2.261 μA and 0.04 μA, respectively. With the obtained I_L (μA) and the above regression equation, the fDNA concentration (*i.e.* LOD) of our biosensor was calculated to be 0.018 fg μL^{-1}. As listed in Table S2 (ESI†), our method exhibited a wide linear range and low LOD, which were comparable with or even superior to those reported in other methodologies for the detection of other avian influenza related viruses and PTP1. This could be attributed to the elaborate design of the electrochemical detection route, which rationally combined the LAMP technique, pH-responsive DiMSs, and ExoIII-assisted DNA walking for signal transduction and signal dual-amplification.

To verify the specificity of our biosensor, we investigated the SWV response of the prepared electrodes with fDNA against PTP1, thrombin (TB) and immunoglobulin G (IgG) as interferents, along with blank (without fDNA) and no-primers (without primers) samples in LAMP. From Fig. 4A, the SWV currents corresponding to PTP1, TB and IgG with the same concentration of 10 pg μL^{-1} were almost the same as the Blank or No-primers samples. However, significantly decreased and almost equal SWV currents were observed for fDNA (1 pg μL^{-1}) and its mixture with PTP1. This indicated that the substitution of fDNA to PTP1, TB and IgG could not promote the LAMP reaction and H^+ ion generation, leading to disabled DiMS assembly and unchanged electrochemical response at the electrode surface. In

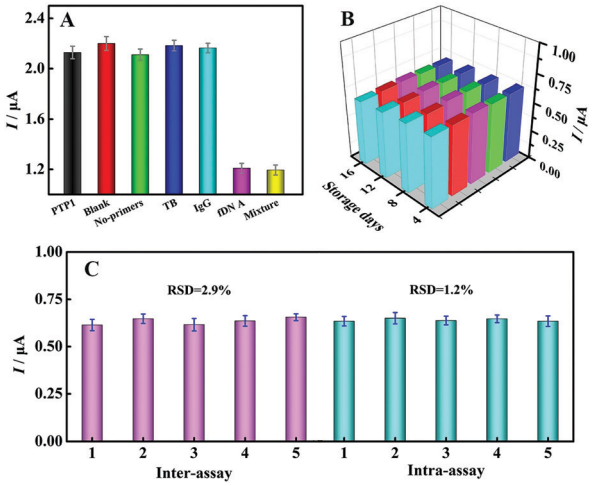

Fig. 4 (A) Specificity of the biosensor with fDNA (1 pg μL^{-1}) against PTP1 (10 pg μL^{-1}), blank, no-primers, TB (10 pg μL^{-1}), IgG (10 pg μL^{-1}) and their mixture. (B) Stability of the biosensor after being stored for 4, 8, 12 and 16 days. (C) Reproducibility of five electrodes prepared in the same batch (inter-assay) and five different batches (intra-assay). Error bars: *s*, $n = 5$.

particular, five electrodes with 1 pg μL^{-1} of fNDA were prepared under the optimized experimental conditions and stored for 4, 8, 12 and 16 days, respectively. After that, the obtained SWV current retained 98.8%, 96.5%, 93.4% and 90.6% of its initial value with a relative standard deviation (RSD) of 3.1% (Fig. 4B). Moreover, from Fig. 4C, five electrodes prepared in the same batch and five different batches under the optimized conditions displayed almost identical SWV responses with 2.9% and 1.2% RSD for the inter-assay and intra-assay, respectively. All the results indicated the good specificity, stability and reproducibility of our method. Moreover, the preliminary applicability of the biosensor was verified by evaluating the fDNA content in human serum samples using the standard addition method, and the result was shown in Table S3 (ESI†).

To conclude, based on fDNA-dependent LAMP-H^+ to induce the pH-responsive DiMS for signal transduction and ExoIII-assisted DNA walking for signal dual-amplification, a simple, specific and ultrasensitive electrochemical biosensor was developed for the detection of the Flu A virus biomarker DNA. Our detection method rationally and elaborately integrated the simplicity and specificity of the LAMP technique, the high pH-responsiveness of DiMS as a signal transducer, and ExoIII-assisted W walking for efficient signal dual-amplification, which, to the best of our knowledge, was utilized for the first time for the electrochemical assay of fDNA. Nevertheless, non-specific nucleotide amplification during the LAMP reaction might result in a background signal to some extent. This work provides another new idea to extend further the extensive application of the LAMP technique *via* combining it with unique DNA nanostructures, especially in biomolecule analysis, disease diagnosis and treatment.

This work was financially supported by the NNSF of China (21775123 and 21775124) and the Natural Science Foundation of Chongqing (cstc2018jcyjAX0214).

Conflicts of interest

There are no conflicts to declare.

Notes and references

1 T. Notomi, H. Okayama, H. Masubuchi, T. Yonekawa, K. Watanabe, N. Amino and T. Hase, *Nucleic Acids Res.*, 2000, **28**, 63e.
2 S. Cai, C. Jung, S. Bhadra and A. D. Ellington, *Anal. Chem.*, 2018, **90**, 8290–8294.
3 H. Yuan, Y. C. Chao, S. S. Li, M. Y. H. Tang, Y. Huang, Y. Che, A. S. T. Wong, T. Zhang and H. C. Shum, *Anal. Chem.*, 2018, **90**, 13173–13177.
4 L. Becherer, M. Bakheit, S. Frischmann, S. Stinco, N. Borst, R. Zengerle and F. V. Stetten, *Anal. Chem.*, 2018, **90**, 4741–4748.
5 C. S. Ball, Y. K. Light, C. Koh, S. S. Wheeler, L. L. Coffey and R. J. Meagher, *Anal. Chem.*, 2016, **88**, 3562–3568.
6 K. Hashimoto, M. Inada and K. Ito, *Anal. Chem.*, 2019, **91**, 3227–3232.
7 S. Roy, N. F. Mohd-Naim, M. Safavieh and M. U. Ahmed, *ACS Sens.*, 2017, **2**, 1713–1720.
8 Y. D. Ma, K. Luo, W. H. Chang and G. B. Lee, *Lab Chip*, 2018, **18**, 296–303.
9 B. J. de Kort, G. A. ten Kate, G. J. de Jong and G. W. Somsen, *Anal. Chem.*, 2011, **83**, 6060–6067.
10 A. Sappat, W. Jaroenram, T. Puthawibool, T. Lomas, A. Tuantranont and W. Kiatpathomchai, *J. Virol. Methods*, 2011, **175**, 141–148.
11 S. B. Xie, Y. L. Yuan, Y. Song, Y. Zhuo, T. Li, Y. Q. Chai and R. Yuan, *Chem. Commun.*, 2014, **50**, 15932–15935.
12 J. M. Zhao, J. X. Gao, T. Zheng, Z. H. Yang, Y. Q. Chai, S. H. Chen, R. Yuan and W. J. Xu, *Biosens. Bioelectron.*, 2018, **106**, 186–192.
13 L. J. Xu, S. N. Hong, N. Sun, K. W. Wang, L. Zhou, L. Y. Ji and R. J. Pei, *Chem. Commun.*, 2016, **52**, 179–182.
14 G. Mata and N. W. Luedtke, *J. Am. Chem. Soc.*, 2015, **137**, 699–707.
15 M. A. S. Abdelhamid, A. J. Gates and Z. E. Waller, *Biochemistry*, 2019, **58**, 245–249.
16 P. Shrestha, Y. X. Cui, J. Wei, S. Jonchhe and H. B. Mao, *Anal. Chem.*, 2018, **90**, 1718–1724.
17 W. H. Chen, X. Yu, A. Cecconello, Y. S. Sohn, R. Nechushtai and I. Willner, *Chem. Sci.*, 2017, **8**, 5769–5780.
18 L. Heinen and A. Walther, *Chem. Sci.*, 2017, **8**, 4100–4107.
19 W. J. Ma, L. A. Yan, X. X. He, T. P. Qing, Y. L. Lei, Z. Z. Qiao, D. G. He, K. H. Huang and K. M. Wang, *Anal. Chem.*, 2018, **90**, 1889–1896.
20 Y. L. Lei, X. X. He, J. L. Tang, H. Shi, D. G. He, L. A. Yan, J. B. Liu, Y. Zeng and K. M. Wang, *Chem. Commun.*, 2018, **54**, 10288–10291.
21 H. A. Assi, M. Garavís, C. González and M. J. Damha, *Nucleic Acids Res.*, 2018, **46**, 8038–8056.
22 I. V. Nesterova and E. E. Nesterov, *J. Am. Chem. Soc.*, 2014, **136**, 8843–8846.
23 M. Q. He, K. Wang, W. J. Wang, Y. L. Yu and J. H. Wang, *Anal. Chem.*, 2017, **89**, 9292–9298.
24 A. M. Fleming, Y. Ding, R. A. Rogers, J. Zhu, J. Zhu, A. D. Burton, C. B. Carlisle and C. J. Burrows, *J. Am. Chem. Soc.*, 2017, **139**, 4682–4689.
25 G. Pelossof, R. Tel-Vered, S. Shimron and I. Willner, *Chem. Sci.*, 2013, **4**, 1137–1144.
26 J. Wang, R. C. Fang, J. Hou, H. C. Zhang, Y. Tian, H. T. Wang and L. Jiang, *ACS Nano*, 2017, **11**, 3022–3029.
27 L. Zou and L. S. Ling, *Anal. Chem.*, 2018, **90**, 13373–13377.
28 J. L. Zhang, X. Wang, Y. Fu, Y. Han, J. Y. Cheng, Y. Q. Zhang and W. Li, *Langmuir*, 2013, **29**, 14345–14350.
29 G. L. Long and J. D. Winefordner, *Anal. Chem.*, 1983, **55**, 712A–724A.

